

Fol. 41 B

Fiskeridirektoratets
Bibliotek

This paper not to be cited without prior reference to the author

International Council for
the Exploration of the Sea

Fish Capture Committee
C.M. 1991/B:36
Ref. Session X

**SCHOOL GEOMETRY MEASUREMENTS USING SONAR
ACCURACY AND AN ALGORITHM FOR SCHOOL DETECTION**

by

Ole Arve Misund

Institute of Marine Research,
Fish Capture Division,
P.O. Box 1870, N-5024 Bergen, Norway.

ABSTRACT

The accuracy of geometric measurements of schools, using horizontal guided single-beam or multi-beam sonar, is simulated. For both types of sonars, the accuracy is dependent of horizontal beam-width and range. As multiple beams do not overlap, the accuracy for multi-beam sonars increases with school size. An algorithm for numeric detection, area measurements, and classification of schools are outlined.

873

INTRODUCTION

When fish are schooling close to surface, use of horizontal guided sonar may be an adequate tool for fish abundance estimation. The biomass estimation may be based on relationships between the geometric dimensions and biomass of schools (Misund et al. 1990; Wheeler and Winters 1990). Use of fisheries sonar for this purpose is not satisfactory (Misund and Floen 1991). This is due both to rather low resolution of the sonar beams and to the fact that post-processing of the recorded targets has to be based on laborious analysis of paper records from single-beam sonars (Halvorsen 1985) or time consuming picture analysis of video records from multi-beam systems (Gunderson et al. 1982; Wilkins 1986).

The increasing interest for acoustic dimensioning of schools has motivated a simulation study to evaluate how the accuracy of geometric measurements depends on the beam characteristics. For single-beam sonars, Johannesson and Losse (1977) showed how the accuracy in measurements of school dimensions is influenced by school size, vessel speed, and stylus thickness of paper recorders. The multi-beam technology gives an instantaneous horizontal projection of a recorded school, but the accuracy is still limited by the beam characteristics. In this study only the effect of the beam-width is considered. This is because at the actual recording range of schools (100 to 500 m away from the vessel), realistic beam-width causes a distortion of a target projection in the order of tens of meter, while the pulse-length distortion is usually less than 10 meters. The simulation also includes the effect of school size in addition to pulse repetition rate for single-beam sonars.

Practical application of horizontal guided sonar for abundance estimation of schooling fish is dependent of algorithms for automatic detection of school targets, especially when applying multi-beam sonar. Storing of digitized data for each ping is a practical solution for the single-beam systems (Hewitt et al. 1976), but for multi-beam systems this principle will result in tremendous amounts of data.

An algorithm for numeric detection of school targets is therefore outlined. The algorithm is based on thresholding of well-defined targets, and can be used as the basis for estimation of school dimensions also.

METHODS

A simple simulation of school dimension measurements, using a horizontal guided, sideways directed, single-beam sonar, is outlined in Figure 1. The sonar emits pulses at intervals (a) from 1 to 9 m (in steps of 2 m) along the track of the vessel. The nominal beam-width (φ) varies from 2° to 12° (-3 db points) in steps of 2° . The school target has a diameter (D) varying from 2 to 50 m (in steps of 2 m), and occurring at a range (R) from 100 to 500 m (in steps of 100 m) to the side of the vessel track. The start position (Y') of the school target varies slightly (within an interval of 10 m in steps of 1 m) to simulate the ping error (Johannesson and Losse 1977). The probability (p) of detecting the school target is 0 if the crosswise extent of the beam in the actual range interval is outside the interval of the school extent, and 1 if inside;

$$p = \begin{cases} 1: Y \pm R \cdot \tan(\varphi/2) \in [Y' - D/2, Y' + D/2] \\ 0: Y \pm R \cdot \tan(\varphi/2) \notin [Y' - D/2, Y' + D/2] \end{cases}$$

According to this, the projected school diameter (cw') will be equal to;

$$cw' = n * a$$

where n is the number of pings with $p = 1$. When correcting for the effect of the beam-width, it is anticipated that the projected school extent can be overestimated by a factor uniformly distributed in the interval $[0, 2R \cdot \tan(\varphi/2)]$. The corrected school diameter (CW) is thereby found by;

$$CW' = cw' - 2 \cdot (R \cdot \tan(\varphi/2) \cdot \text{uniform})$$

where "uniform" is a function (SAS 1988) that generates a number uniformly distributed in the interval $[0,1]$.

School dimension measurements by multi-beam sonar are simulated as shown in Figure 2. The sonar beam, with a width varying from 2° to 12° , is anticipated to rotate anticlockwise

from 0 to $\pi/2$. This simulates the rotational directional transmission (RDT) principle applied on several multi-beam sonars. The school is positioned at a range (R) varying from 100 to 500 m in steps of 100 m, and at an angle, varying from 41° to 49° in steps of 2° . The school diameter (D) is varying from 2 to 50 m in steps of 2 m.

Detection of the school is based on the position of the school projection in the Y-direction relative to the beam projection in the Y-direction. Y' is the lower and Y'' is the upper limit of the school projection, and Y_{\max} and Y_{\min} are the upper and lower limits of the beam projected in the Y-direction;

$$\begin{aligned} Y' &= R' \cdot \sin(\beta - \alpha) \\ Y'' &= R' \cdot \sin(\beta + \alpha) \end{aligned}$$

If the school diameter is less than the crosswise extent of the beam, the detection probability (p^*) is expressed by;

$$D < 2 \cdot R \cdot \tan(\varphi/2): p^* = \begin{cases} 1 : Y_{\max} > Y'' \text{ and } Y_{\min} < Y' \\ 0 : \text{all other cases} \end{cases}$$

If the school diameter is larger than the crosswise extent of the beam, the detection probability is split in to three categories (p_1, p, p_2), depending on which part of the school that is detected. In this case we have;

$$\begin{aligned} D > 2 \cdot R \cdot \tan(\varphi/2): \quad p_1 &= \begin{cases} 1 : Y_{\max} > Y' \text{ and } Y_{\min} < Y' \\ 0 : \text{all other cases} \end{cases} \\ p &= \begin{cases} 1 : Y_{\max} < Y'' \text{ and } Y_{\min} > Y' \\ 0 : \text{all other cases} \end{cases} \\ p_2 &= \begin{cases} 1 : Y_{\max} > Y'' \text{ and } Y_{\min} < Y'' \\ 0 : \text{all other cases} \end{cases} \end{aligned}$$

If the school diameter is less than the crosswise extent of the beam, the recorded school diameter is found by;

$$CW' = 2 * R * \tan(\varphi/2) * \text{uniform} = b$$

assuming that the projected school extent is overestimated by a factor uniformly distributed in the interval $[0, 2R * \tan(\varphi/2)]$. If the school diameter is larger than the crosswise extent of the beam, the recorded school diameter is found by;

$$CW' = 2 * R * n * \tan(\varphi/2) + n_1 * b + n_2 * b$$

where n , n_1 , and n_2 correspond to the number of pings that p , p_1 , and $p_2 = 1$.

Both for the single-beam and multi-beam simulation, the accuracy of the recorded school diameter is expressed by:

$$\text{absolute error} = CW' - D$$

$$\text{relative error} = (CW' - D)/D$$

SIMULATION RESULTS

The average absolute error is clearly dependent of horizontal beamwidth of horizontal beamwidth, both when simulating single-beam and multi-beam sonar (Fig. 3). For a school diameter of 2 m, the average absolute error increases from about 2 m to about 30 m for a beam-width of 2° and 12°, respectively. An important difference in the resolution capabilities of the two sonar systems is, however, that while the average absolute error for a given beamwidth is independent of schools size when simulating the single-beam system, the average absolute error decreases with increasing school size irrespective of the beam-widths simulated for the multi-beam system (Fig. 3). The relative error decreases rapidly with increasing school size for both sonar systems, however, but fastest for the multi-beam system (Fig. 4).

Irrespective of beam-width, the absolute error increases with increasing range (Fig. 5). For the multi-beam system, the absolute error for a given range decreases with increasing school size, which is not the case for the single-beam system. Similarly as for the beam-width, the relative error for various ranges decrease rapidly with increasing school size for both sonar systems, but fastest for the multi-beam system (Fig. 6).

The reason for the effect of school size on the absolute error considerations for varying beam-widths and ranges for the multi-beam system is that multiple beams are not assumed to overlap. Consequently, the larger the crosswise school extent relative to the beam-width, the smaller the effect of the beam-width correction, and the better the accuracy.

SCHOOL DETECTION ALGORITHM

Hewitt et al. (1976) has outlined an algorithm for automatic school detection by single-beam sonar. Numeric detection of schools by multi-beam sonar can be based on the same principles by point sampling and digitizing of the echo signal amplitudes at a certain point sampling frequency. This gives a sonar matrix that contains a numeric picture of the echo signal amplitudes along each beam (Fig. 7). The horizontal resolution will be determined by beam-width, range, pulse-length and point sampling frequency. The principle for numeric school detection can be;

Threshold (TV): point sample bigger than average noise and reverberation level (after amplitude adjustment by automatic gain control (AGC) and filtering).

Echo-line: a certain number of succeeding point samples (bigger than the smallest defined lengthwise school extent) which is $> TV$ and limited by a certain number of preceding or following point samples $< TV$.

Echo-block: a certain number of adjacent echo-lines (bigger than smallest defined crosswise school extent) that is limited by signal levels $< TV$ in the neighbouring beams.

School: echo-block that is found in at least two succeeding pings and in about the same position relative to the vessel (ping-to-ping movement less than maximum swimming speed).

The threshold-value (TV) should be adjustable and chosen on the basis of the sonar conditions given. For every ping there must be searched for recordings that fulfil first the echo-line and then the echo-block criteria. If targets are accepted, the sonar matrix for the actual ping must be compared to that for the preceding ping to test if the school criteria is fulfilled. If a target is categorized as a school, the sonar matrix for the last ping should be stored temporarily for post-processing.

Stored "school"-targets should be viewed successively during a "judging"-session for final classification. For targets "judged" as schools, an estimate of the school area (A) should be calculated. The area of the edge elements (A'_{ij}) in the school matrix can be corrected stochastically by using the proportion between the amplitude (V_{ij}) in the edge element and the average amplitude (\bar{V}_{Rj}) in the real school matrix elements with the same range coefficient;

$$A'_{ij(\text{corr})} = A'_{ij} * V_{ij} / \bar{V}_{Rj}$$

$$\text{School area (A)} = A_{ij} + A'_{ij(\text{corr})}$$

CONCLUSION

Multi-beam sonar is favourable for school geometry measurements as the horizontal school extent is projected instantaneously. Because the multiple beams do not overlap, the absolute accuracy improves with the extent of the school, which is not the case for single-beam sonar.

A narrow horizontal beam-width is necessary for geometry measurements of small schools with an acceptable level of accuracy. In the range interval simulated (100 - 500 m), a multi-beam sonar, having a beam-width of 2° , overestimates the diameter of a 10 m wide school by about 20 % in average.

REFERENCES

- Gunderson, D. R., G. L. Thomas and P. J. Cullenberg. 1982. Combining sector scanning sonar and echosounder data from echo surveys. ICES/FAO Symposium on Fisheries Acoustics, Bergen, Norway, 21-24 June, 1982. Doc. no. 101.
- Halvorsen, H. 1985. En vurdering av mulighetene for mengdemåling av pelagisk stimfisk med horisontalt rettet sonar [An evaluation of the possibilities of abundance estimation of pelagic schooling fish by horizontal guided sonar]. Thesis, Inst. of Fisheries Biology, University of Bergen, Bergen, Norway, 1985. (In Norwegian.)
- Hewitt, R., P. E. Smith and J. C. Brown. 1976. Development and use of sonar mapping in the California current. Fish. Bull., U. S., 74: 281-300.
- Johannesson, K. A. and G. F. Losse. 1977. Methodology of acoustic estimations of fish abundance in some UNDP/FAO Resource survey Projects. Rapp. p.-v. Reun. Cons. int. Explor. Mer, 170: 296-318.
- Misund, O. A. and S. Floen. 1991. Abundance estimation of fish schools using a fisheries sonar. ICES C.M. 1991/B:35.
- Misund, O. A., A. Aglen, A. K. Beltestad and J. Dalen. 1990. Relationships between the geometric dimensions and biomass of schools. ICES C.M. 1990/B:41.
- SAS 1988. SAS Institute Inc. SAS Language Guide, Release 6.03 Edition. Cary, NC: SAS Institute Inc., 1988. 530 pp.
- Wilkins, M. E. 1986. Development and evaluation of methodologies for assessing and monitoring the abundance of widow rockfish, *Sebastes entomelas*. Fish. Bull., U. S., 84: 287-310.

Wheeler, J. P. and G. H. Winters. 1990. The development of hydroacoustic techniques for the empirical estimation of biomass for Newfoundland herring stocks. Proc. int. Herring Symposium, Oct. 1990, Anchorage, Alaska. pp. 145-162.

Single-beam

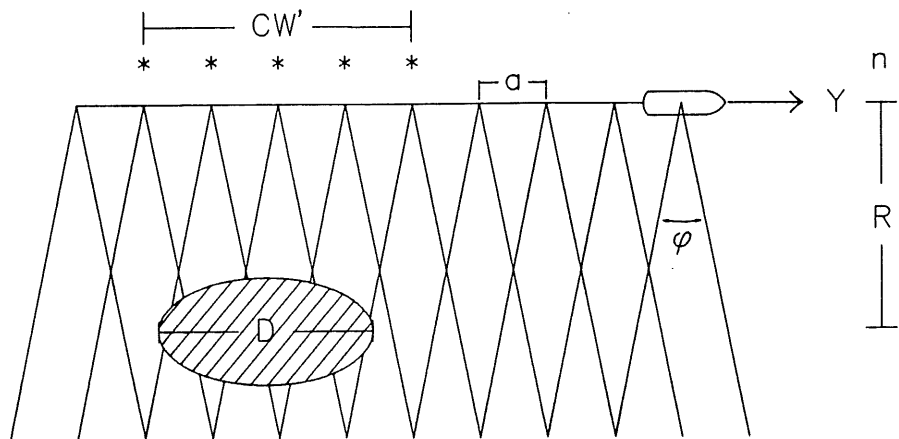


Figure 1. Measurement of school diameter (D) using a horizontal guided, sideways directed single-beam sonar (cw' : projected crosswise school extent, a : pulse repetition rate, R : range, ϕ : beam-width, *: pings in which the school is detected).

Multi-beam

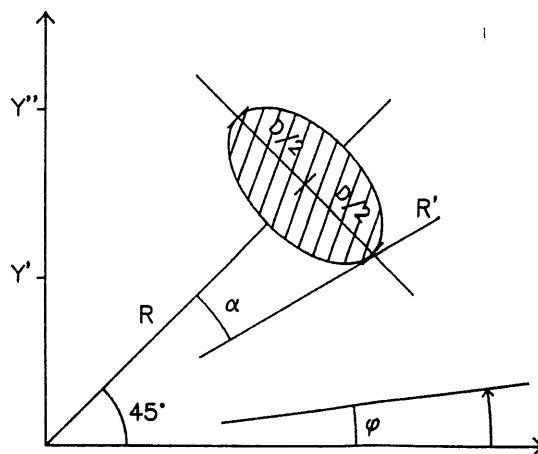


Figure 2. Measurement of school diameter (D) using multi-beam sonar (ϕ : beam-width, R : range, see text for more explanation).

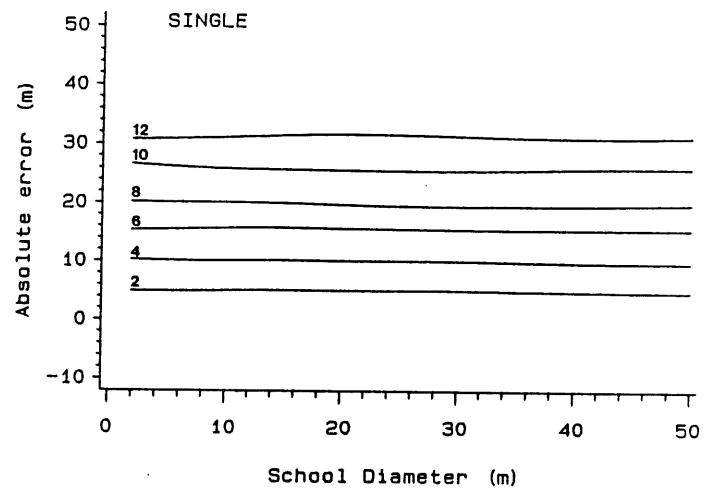
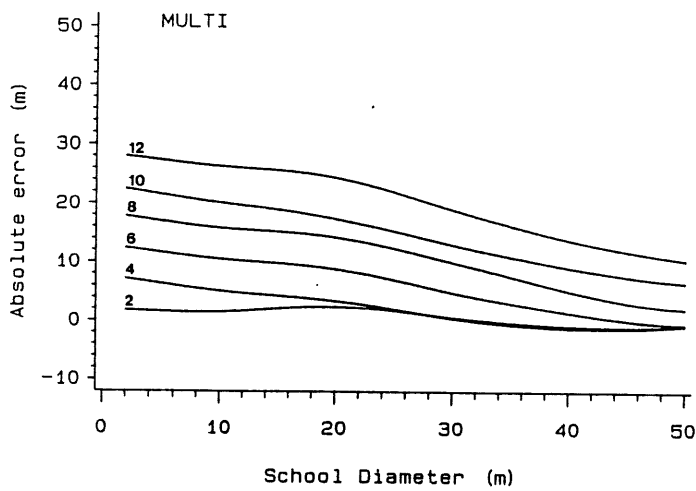


Figure 3. Average absolute error when simulating school diameter measurements by multi-beam and single-beam sonar for various beam-widths.

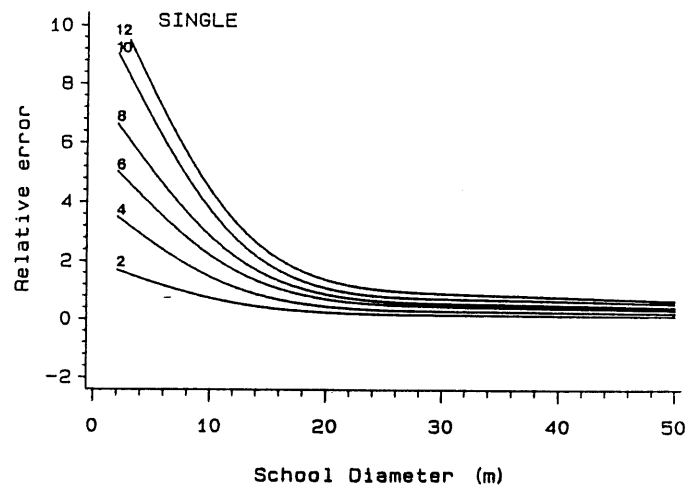
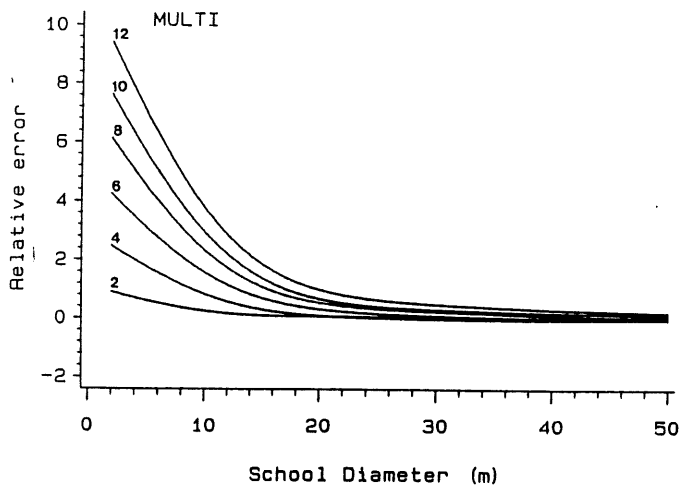


Figure 4. Average relative error when simulating school diameter measurements by multi-beam and single-beam sonar for various beam-widths.

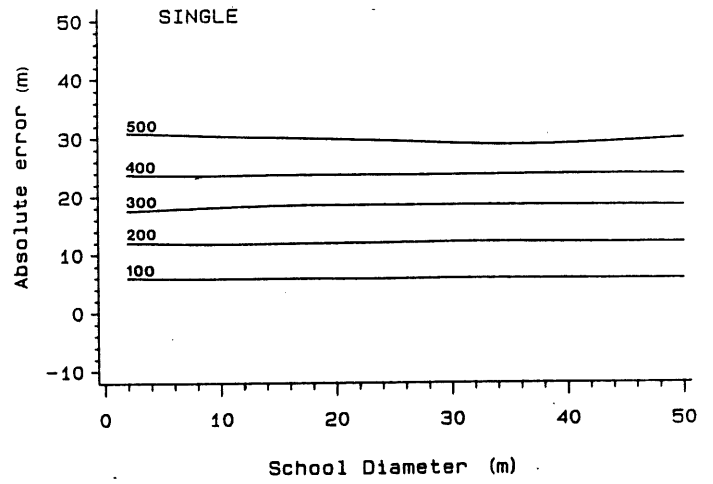
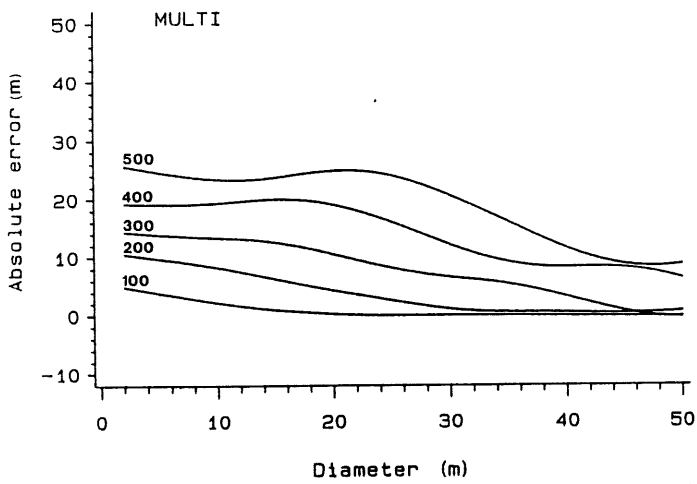


Figure 5. Average absolute error when simulating school diameter measurements by multi-beam and single-beam sonar for varying ranges vessel-to-school.

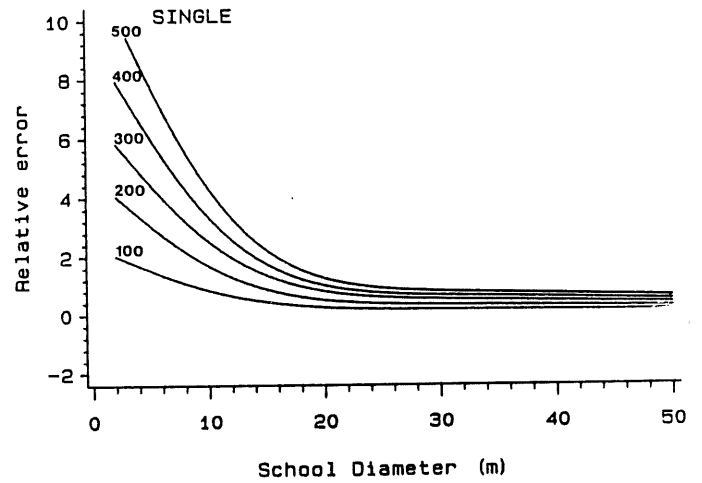
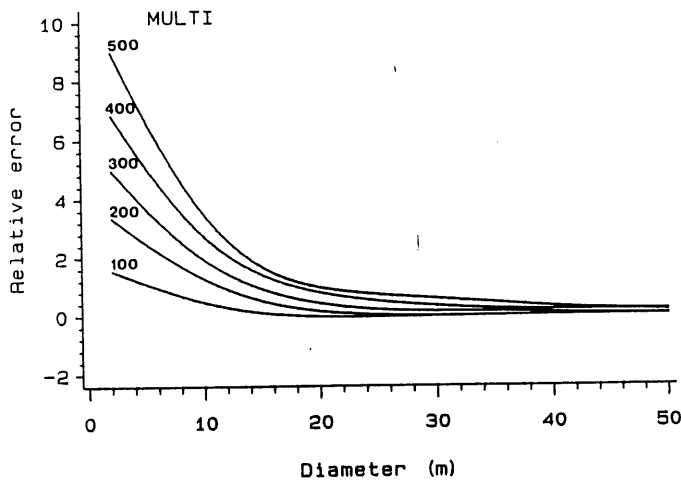


Figure 6. Average relative error when simulating school diameter measurements by multi-beam and single-beam sonar for varying ranges vessel-to-school.

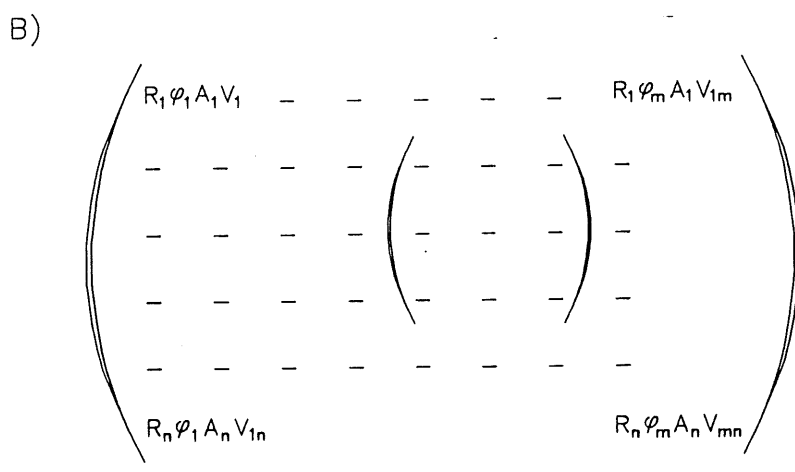
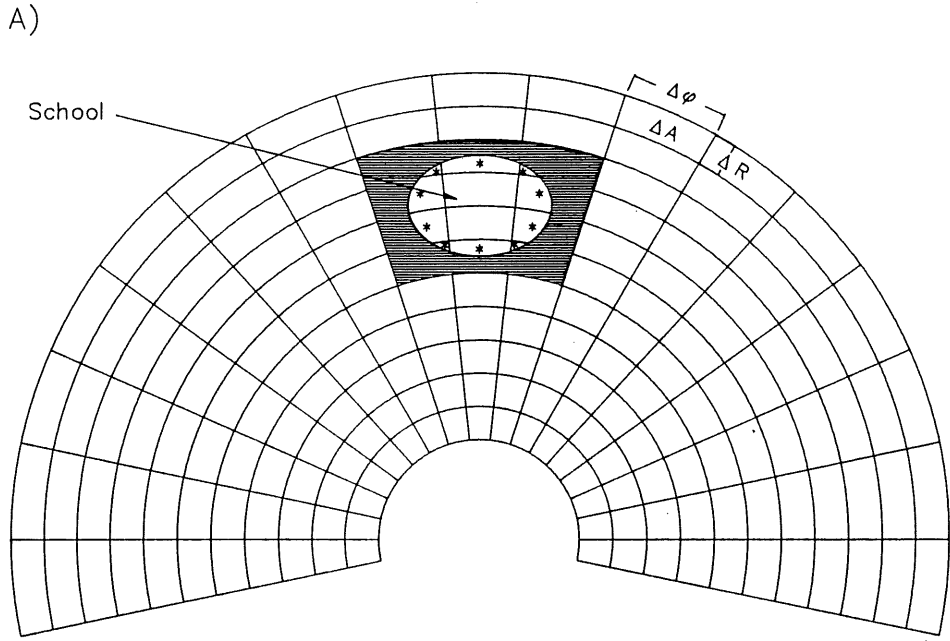


Figure 7. A) Sonar projection of elliptical school (ΔR : range interval, $\Delta\phi$: horizontal beam width, ΔA : area for element ij , *: edge element). The hatcure shows the distortion due to beam width and pulse-length. B) Sonar matrix where the central elements represents a school. Known coefficients: R (range), ϕ (beam width), A (area). Variable: V (signal amplitude).